Integrated Terahertz High-Speed Data Communication and High-Resolution Radar Sensing System Based-on Photonics

Yanyi Wang (1), Feng Zhao(2), Kaihui Wang(1),Jiao Zhang (3) , Mingzheng Lei(3), Min Zhu(3), Cuiwei Liu(1), Li Zhao(1), Junjie Ding(1), Wen Zhou(1), and Jianjun Yu(1)

(1) Fudan University, Shanghai, China * jianjun@fudan.edu.cn

(2) Xi'an University of Posts and Telecommunications, Xi'an, 710121, China

(3) Purple Mountain Laboratories, Nanjing, Jiangsu 211111, China

Abstract *We propose and demonstrate a new architecture that integrates terahertz high-speed data communications and high-resolution radar sensing systems. Based on THz photonics for the first time, we realize THz communication data transmission at THz band, while achieving two target detections.*

Introduction

With the evolution of 5G mobile communication to 6G, it is expected that in the future, 6G network will become the "nerve center" connecting the physical world and the digital world while having strong communication capabilities. 6G extends the access of network end to things, and the vision of all things intelligence becomes a reality, which will age into intelligence. As one of the potential 6G technologies, the integration of communication and radar sensing is a research hotspot in future 6G technology [1-5]. Terahertz (THz) communication, as a promising candidate technology in the future 6G, has the advantages of abundant spectrum resources and ultra-fast data rate [6-8]. The integration of THz communication and radar sensing will be one of the key technologies in future 6G immersive applications. Unfortunately, only a few reports on the integration of communications and radar sensing, has been reported so far, especially in the THz domain. In [9], based on photonics-aided THz, a joint data communication and radar sensing system is proposed. Here, actually, the function of our called 'sensing' is not really realized without the recognition of echo signal. In [10], a unified data communication and radar sensing system using photonics technology is proposed. Unfortunately, the data rate is relatively low and the carrier frequency is as low as 28GHz. In this paper, we propose and experimentally demonstrate a new scheme of THz high-speed data communication and high-resolution radar sensing integrated system with the aid of photonics. We successfully achieve 14-Gbaud QPSK, and 8-Gbaud 16QAM format signals over 1-m wireless transmission, which means that a rate of 32 Gbit/s in the THz communication can be realized below the soft-decision forward error correction (SD-FEC) threshold of 2.4 × 10^{-2}. Simultaneously, for the THz radar sensing, a linear frequency modulated (LFM) signal is established with a range resolution of 3.8 cm. Two targets which are 30cm and 40cm away from the reference position are successfully detected. To the best of our knowledge, it is for the first time to realize the integrated high-speed data communication and high-resolution radar sensing at the THz band.

Principle and experimental setup

As shown in Fig.1 (a), in-phase/quadrature (I/Q)

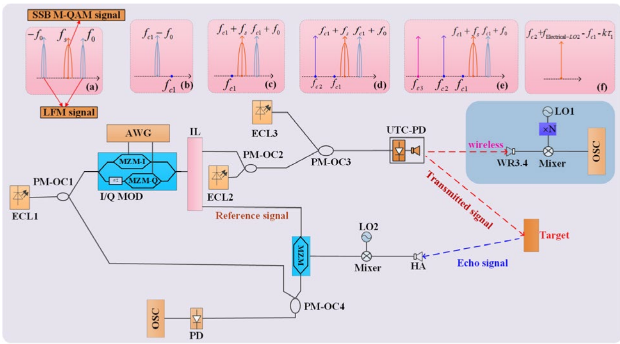

Fig.1: Principle of photonics-based THz high-speed data communication and high-resolution radar sensing integrated system.

modulator is driven by the frequency division multiplexed (FDM) USB RF M-QAM format signal and DSB IF LFM signal. The instantaneous frequency of the IF-LFM signal can be expressed as $f_{IF}(t) = f_0 + kt$, where f_0 is the initial frequency and k is the chirp rate. The modulated signal after the I/Q modulator is divided into two paths by IL, as shown in Fig.1 (b) and Fig.1 (c), respectively. The lower path is used as the reference signal for radar sensing. The upper path is then coupled with ECL-2 operated as an optical local oscillator (OLO1) through PM-OC2, as shown in Fig.1 (d). The coupled signal then is coupled with another ECL-3 operated as OLO2 through PM-OC3, as shown in Fig.1 (e). At last, the coupled optical signal from PM-OC3 is used to simultaneously generate communication and

978-1-6654-3868-1/21/$31.00 ©2021 IEEE

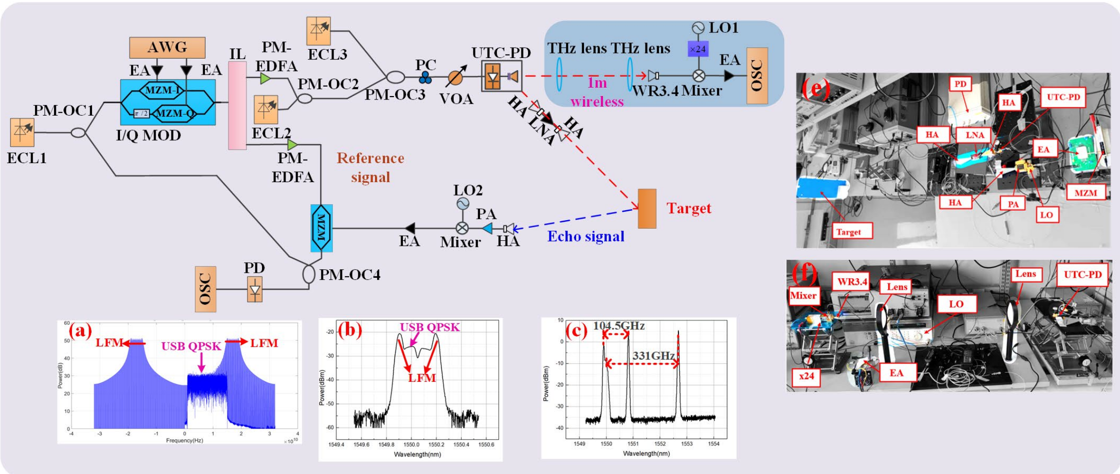

Fig. 2: The experimental setup of the photonics-based THz high-speed data communication and high-resolution radar sensing integrated system. Photos of: (e) the photonics-based THz high-resolution sensing signal system setup, and (f) photonics-based THz high-speed data communication system setup.

sensing signals after heterodyne beating at the UTC-PD end. After wireless transmission, the THz M-QAM format signal is down-converted and captured by the digital OSC. The reflected echo signal is converted into the IF domain to drive MZM at its minimum transmission point to modulate the reference signal. The modulated optical signal after MZM is coupled with ECL-1 by PM-OC4. After PD conversion, the electrical signal is captured. At this point, as shown in Fig.1 (f). The de-chirped signal has a frequency of $f_{c1} - f_{c2} - f_{ELO2} + k\tau$, where τ is the time delay of the reflected LFM signal compared with the transmitted signal. The distance measurement between the two positions can be achieved by calculating the frequency difference between the two positions as: $d = c\Delta\tau / 2 = c\Delta f / 2k$.

Fig. 2 shows the experimental setup of our proposed photonics-based THz high-speed data communication and high-resolution radar sensing integrated system. A 1550.32-nm lightwave is emitted from an ECL1 with ~100kHz linewidth, which is divided into two paths through a 50:50 PM-OC1. The upper path is sent to the I/Q modulator with a 3-dB optical bandwidth of 25GHz as the optical carrier. 7-GHz USB signal carrying 14-Gbaud QPSK transmitted data and 17.5-GHz LFM signal with a bandwidth of 5GHz and temporal period of 10-9s are generated via offline MATLAB programming. 14-Gbaud QPSK waveform is a pulse shaped with a root-raised-cosine filter with a roll-off factor of 0.01. The USB QPSK signal and DSB LFM signal are frequency division multiplexed, as shown in Fig. 2 (a). Then, the FDM-based signal is converted into analog signal by an AWG, which has a sampling rate of 64-GSa/s. The analog signal is amplified by an electrical amplifier (EA) with a bandwidth of 25GHz to drive the I/Q modulator. Then the optical carrier signal is modulated with QPSK and LFM signal after the I/Q modulator as shown in Fig2. (b). After the I/Q modulator, the modulated signal is divided into two paths by an IL with a frequency space of 50GHz. After amplified by a PM-EDFA, the USB QPSK signal and LFM signal are coupled with ECL-2 at a wavelength of 1551.01 nm by PM-OC2. And then the optical signal after PM-OC2 is coupled with ECL-3 at a wavelength of 1552.93 nm by PM-OC3, as shown in Fig2. (c). Then, a polarization controller (PC) is placed after the PM-OC3 to control the polarization state. A variable optical attenuator (VOA) is placed after the PC to control the power into UTC-PD. The THz LFM signal and QPSK communication signal are simultaneously generated by optical heterodyne beating at the output of UTC-PD. For the THz LFM signal transmission and reception, as shown in Fig2. (f), at the output of the UTC-PD, the THz LFM signal is simultaneously generated at 104.5-GHz (17.5+87=104.5) and 341.5-GHz (17.5+324=341.5) bands. Due to the transmission loss increasing with the frequency, we choose the 104.5-GHz band for radar sensing. We replace the THz amplifier with a pair of HAs with a gain of 25dBi and an LNA with a gain of 20dB, as shown in Fig. 2. The reflected echo signal is received by HA with a gain of 25dBi and is properly amplified by a power amplifier (PA) with a gain of 25dB before down-converted into the IF domain. Then, the received echo signal is down-converted into the IF domain by an 83.5-GHz sinusoidal RF source and a commercial balanced mixer. After down-conversion, the echo signal is amplified by another EA with 25-dB gain before driving the MZM. The reference optical signal from the lower path IL is modulated by the echo signal. The modulated signal is coupled with the lower path optical carrier from the PM-OC1 by PM-OC4. At last, the optical signal is sent to a 3-dB bandwidth of 20-GHz PD. After PD, the generated electrical signal is detected by an OSC with a 100-GSa/s sampling rate and 33-GHz bandwidth. For the communication data transmission and reception, as shown in Fig2. (f), the QPSK signal is also simultaneously generated at the frequency of 94-GHz (87+7=94) and 331-GHz (324+7=331). To verify the THz data transmission, we select the 331GHz band for communication, and then the THz QPSK signal is delivered over a 1-m free-space wireless link. A pair of THz lenses are used to focus the THz signal. At the receiver side, the received THz signal is down-converted into the IF domain by using a THz WR3.4 mixer operating at the 300–360-GHz band, driven by a 24-time frequency multiplied electrical LO1 signal of 13.4GHz. The down-converted 9-GHz IF signal is amplified by another EA with 25-dB gain, and then fed into an OSC, for subsequent digital signal processing (DSP) including down-converted, orthogonalization, constant modulus algorithm equalization (CMA), frequency offset estimation (FOE), and carrier phase estimation (CPE) [11].

Experimental results and discussions

The de-chirped signal is captured by the OSC. The range resolution of the 5GHz bandwidth radar is theoretically as high as 3.8cm. Fig. 3 (c) gives the combined electrical spectrum of the QPSK transmission signal and LFM signal. Fig. 3(d) gives the measured BER performance versus the input power into the UTC-PD for the QPSK modulation format signal. As shown in Fig. 3(d), for both 12-Gbaud and 14-Gbaud QPSK cases, when the input power into the UTC-PD is larger than 8dBm, the BER can be less than the 20% SD-FEC threshold of 2.4×10^{-2}. Therefore, the 28Gbit/s is achieved. Inset in Fig. 3 (d) shows the QPSK constellation for the 14-Gbaud transmission. Fig.3 (e) gives the combined electrical spectrum of the 16QAM transmission signal and LFM signal. Fig. 3(f) gives the measured BER performance versus the input power into the UTC-PD for the 16QAM format signal. As shown in Fig. 3(f), for both 6-Gbaud and 8-Gbaud 16QAM cases, when the input power into the UTC-PD is larger than 10dBm, the BER can be less than the 20% SD-FEC threshold of 2.4×10^{-2}. Therefore, the rate of 32Gbit/s is achieved. Inset in Fig. 3 (f) shows the 16QAM constellation for the 8-Gbaud transmission.

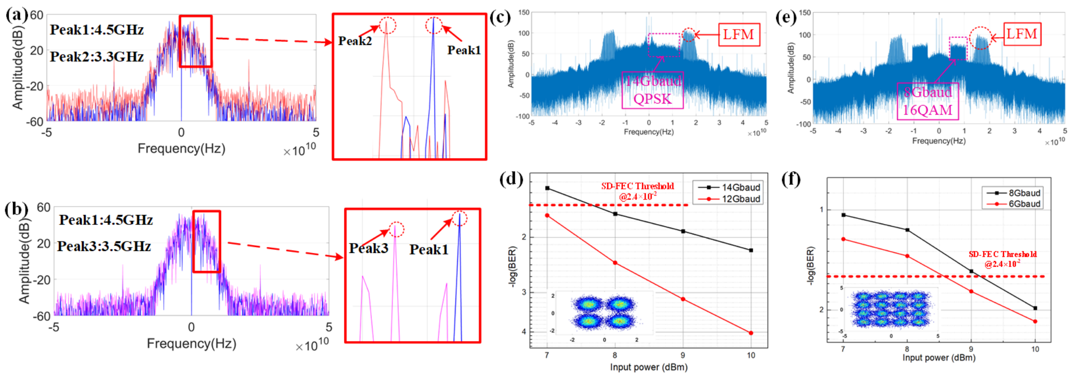

Fig. 3:(a) and (b) Spectra of the de-chirped signal for 40cm and 30cm away from the reference position, respectively. (c) The combined electrical spectrum of QPSK transmission signal and LFM signal. (d) BER versus input power into UTC-PD for the QPSK signal. (e) The combined electrical spectrum of 16QAM transmission signal and LFM signal. (f) BER versus input power into UTC-PD for the 16QAM signal.

Figs.3 (a) and (b) show the spectra of the de-chirped signal after executing FFT. As can be seen from Fig.3(a), there are two clearly separated spectral peaks located at 4.5GHz and 3.3GHz, respectively. The peak1 spectra correspond to the reference position. Based on Ref [12], the distance between the two positions is proportional to the frequency spacing between the two spectral peaks after de-chirping. In this case, the distance between the two positions is calculated to be 36 cm, which is close to the practical value. Next, the metal target away from the 30cm reference position is tested, as shown in Fig.3(b). Based on Ref [12], the distance between the two positions is calculated to be 30 cm, which is equal to the practical value. Therefore, the measurement errors are 4 cm and 0 cm, respectively.

Conclusions

As a conclusion, we propose and experimentally demonstrate a new architecture of photonics-based THz high-speed data communication, and high-resolution radar sensing integrated system. Based on photonics technology, the communication signal and LFM signal are simultaneously generated from one UTC-PD at the THz band. The experimental results show that the rate of 32Gbit/s has been successfully transmitted over a 1-m wireless link at 324GHz band, and at the same time, two targets which are 30cm and 40cm away from the reference position are successfully detected. We believe the proposed architecture is expected to be promising in future 6G communications.

References

[1] H. Viswanathan and P. E. Mogensen, “Communications in the 6G era”, IEEE Access, vol. 8, pp. 57063-57074, 2020.

[2] M. N. Patwary, S. J. Nawaz, M. A. Rahman, S. K. Sharma, M. M. Rashid and S. J. Barnes, “The potential short- and long-term disruptions and transformative impacts of 5G and beyond wireless networks: Lessons learnt from the development of a 5G testbed environment”, IEEE Access, vol. 8, pp. 11352-11379, 2020.

[3] Z. Zhang, et al., “6G wireless networks: Vision requirements architecture and key technologies”, IEEE Veh. Technol. Mag., vol. 14, no. 3, pp. 28-41, 2019.

[4] K. David and H. Berndt, “6G vision and requirements: Is there any need for beyond 5G?”, IEEE Veh. Technol. Mag., vol. 13, no. 3, pp. 72-80, 2018.

[5] T. Wild, V. Braun and H. Viswanathan, “Joint Design of Communication and Sensing for Beyond 5G and 6G Systems,” in IEEE Access, vol. 9, pp. 30845-30857, 2021.

[6] S. Jia, L. Zhang, S. Wang, W. Li, M. Qiao, Z. Lu, N.M. Idrees, X.Pang, H. Hu, X. Zhang, L.K. Oxenløwe, and X. Yu, “2 × 300 Gbit/s Line Rate PS-64QAM-OFDM THz Photonic-Wireless Transmission,” J. Lightwave Technol. vol. 38, no.17, pp. 4715-4721, 2020.

[7] L. Zhang, M. Qiao, S. Wang, Z. Lu, L. Zhang, X. Pang, X. Zhang, and X. Yu, “Nonlinearity-aware optoelectronic terahertz discrete multitone signal transmission with a zero-bias diode,” Opt. Lett. vol. 45, no.18, pp. 5045-5048 ,2020.

[8] S. -R. Moon, M. Sung, J. K. Lee and S. -H. Cho, “Cost-Effective Photonics-Based THz Wireless Transmission Using PAM-N Signals in the 0.3 THz Band,” in Journal of Lightwave Technology, vol. 39, no. 2, pp. 357-362, 2021.

[9] S. Ja et al., “A unified system with integrated generation of highspeed communication and high resolution sensing signals based on THz photonics,” J. Lightw. Technol., vol. 36, no. 19, pp. 4549–4556, 2018.

[10] L.Huang, R.Li, S.Liu, P.Dai, and X.Chen , “Centralized fiber-distributed data communication and sensing convergence system based on microwave photonics,” J. Lightw. Technol., vol. 37, no. 21, pp. 5406–5416, 2019

[11] J. Yu and X. Zhou, “Ultra-high-capacity DWDM transmission system for 100G and beyond,” Commun. Mag. vol. 48, no. 3, pp. S56-S64, 2010.

[12] F. Zhang, Q. Guo, Z. Wang, P. Zhou, G. Zhang, J. Sun, and S. Pan, “Photonics-based broadband radar for high resolution and real-time inverse synthetic aperture imaging,” Opt. Express, vol. 25, no 14, pp. 16274-16281,2017.